Table I. Energy splittings (in eV) and effective electron mass of cubic ZnS as calculated by the KKR method and by CB in comparison with the experimental values found by Cardona and Harbeke,[4] by Baars,[a] and by Kukimoto.[b] The values given in parentheses are those that were fitted by CB. They originate from the same experiments but were extrapolated to $T=0$. The lattice constant used in our calculation as well as by CB is related to room temperature.

Transition	KKR	Experiment	CB[c]
Γ_{15}-Γ_1	3.7	3.71	3.7
		(3.8)	
Γ_{15}-L_1	5.3		5.3
Γ_{15}-X_1	5.8		5.2
Γ_{15}-Γ_{15}	9.0	8.4[a]	8.9
X_5-X_1	7.2	7.03	6.7
		(6.8)	
X_5-X_3	7.5	7.35	7.5
		(7.3)	
X_1-X_3	0.3	0.32	0.8
		(0.5)	
L_3-L_1	5.9	5.82	5.8
		(5.9)	
L_3-L_3	9.9	9.65	9.2
		(9.5)	
m_e^*	$(0.35\text{-}0.40)m_0$	$(0.39\pm0.01)m_0$[b]	$<0.35m_0$

[a]H. Gobrecht and J. Baars, to be published.
[b]H. Kukimoto et al., Phys. Letters 19, 551 (1965).
[c]Cohen and Bergstresser, Ref. 2.

data. Since the method is able to exhibit bands originating from atomic levels as well as free-electron bands, one can use it to decide what kind of interpolation scheme is suitable if one wants to know the energy throughout the Brillouin zone. Moreover, the KKR method (like the APW method) has been modified to include spin-orbit coupling and relativistic effects (see, e.g., Treusch and Roessler[11]). So we hope that this method will be helpful in semiconductor research as it was in the theory of metals.

[1]F. Herman, R. L. Kortum, C. D. Kuglin, and R. A. Short, J. Phys. Soc. Japan Suppl. 21, 7 (1966).
[2]M. L. Cohen and M. H. Bergstresser, Phys. Rev. 141, 789 (1966).
[3]J. Treusch and R. Sandrock, Phys. Status Solidi 16, 487 (1966).
[4]M. Cardona and G. Harbeke, Phys. Rev. 137, A1467 (1965).
[5]J. C. Phillips, J. Phys. Soc. Japan Suppl. 21, 3 (1966).
[6]U. Roessler and M. Lietz, Phys. Status Solidi 17, 597 (1966).
[7]F. Herman and S. Skillman, Atomic Structure Calculations (Prentice Hall, Inc., Englewood Cliffs, New Jersey, 1963).
[8]H. Kukimoto et al., Phys. Letters 19, 551 (1965).
[9]Of course, not all of the transitions given in Ref. 4 are necessarily conclusive, but the gap seems to be. The latter is the only experimental value underlying our calculations. A more detailed discussion will be possible when more results are available concerning other II-VI and III-V compounds.
[10]J. C. Phillips, Solid State Phys. 18, 99 (1966).
[11]J. Treusch, Phys. Status Solidi 19, 603 (1967); U. Roessler, Solid State Commun. 5, 45 (1967).

TWO-MAGNON LIGHT SCATTERING IN ANTIFERROMAGNETIC MnF_2

P. A. Fleury and S. P. S. Porto
Bell Telephone Laboratories, Murray Hill, New Jersey

and

R. Loudon
Physics Department, Essex University, Colchester, England
(Received 9 February 1967)

The strength, line shapes, polarization selection rules, and magnetic field behavior of two-magnon light scattering in antiferromagnetic MnF_2 are reported, and they are interpreted in terms of an excited-state exchange coupling between sublattices and the magnon dispersion relation

We present theoretical and further experimental[1] results on the second-order scattering of light by magnons in antiferromagnetic MnF_2. The two-magnon spectra are interpreted using the known magnon density of states and a new mechanism for light scattering based on excited-state exchange interactions between the two magnetic sublattices. The theory satisfactorily explains (1) the polarization selection rules governing the scattering, (2) the behavior of the scattering in applied magnetic fields, (3) the relation of the sharp features

in the second-order spectra to the critical points in the magnon density of states, and (4) the magnitude of the two-magnon scattering, which is surprisingly large relative to the one-magnon scattering. These results comprise the first complete quantitative interpretation of a second-order Raman spectrum, based on the neutron-measured dispersion relation.

An experimental arrangement similar to that in Ref. 1 was employed. The experimental geometry is indicated by the letters in Fig. 1. For example, "xz" means that the incident light was linearly polarized in the "x" direction, while the scattered light observed was polarized parallel to the crystal c axis in the "z" direction.

The two-magnon spectra of MnF_2 at ~10°K are shown in Fig. 1. A single, rather sharp peak appears in both the "xy" and the "xz" spectra. The "xx" spectrum is broad, weak, and featureless, and has accordingly not been included in Fig. 1. The "xy" peak is centered at 98 cm^{-1}, is rather symmetric, and has a full width at half-maximum of about 4 cm^{-1}, of which about 2 cm^{-1} is instrumental. The "xz" peak is noticeably asymmetric, having

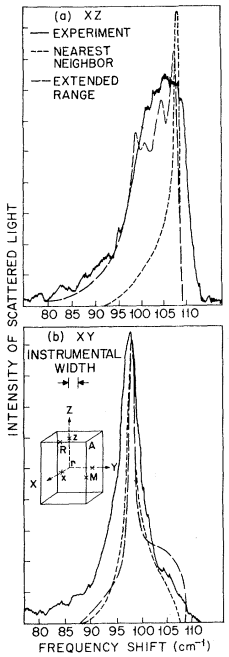

FIG. 1. Theoretical and experimental spectra for second-order magnon scattering in MnF_2 at 10°K. Intensity of theoretical curves are normalized to experiment. (a) "xz" experimental geometry, and (b) "xy" experimental geometry; inset shows Brillouin zone and critical points.

a high-frequency cutoff at about 100 cm^{-1} and a width of about 12 cm^{-1}. The integrated intensities of the two spectra are comparable, the extinction coefficient h being of order 10^{-12} cm^{-1} sr^{-1} in both cases. This is of the same magnitude as the previously observed two-magnon scattering in FeF_2, where the second-order process[2] is 2-3 times stronger than the first-order process.[1]

As in the two-phonon Raman effect, momentum conservation requires that the two magnons which scatter the light have essentially equal and opposite wave vectors ($\vec{k}$ and $-\vec{k}$) and hence equal frequencies, since $\omega_{\vec{k}}=\omega_{-\vec{k}}$. In the absence of external fields the magnon dispersion curve in MnF_2 has a single doubly degenerate branch. The frequency associated with the pair of magnons for a given $\vec{k}$ is thus unique, and interpretation of the two-magnon spectra is much simpler than is usually the case for phonons. The shift in frequency of the scattered light should range between $2\omega_\Gamma$ and $2\omega_Z$ [the subscripts refer to points in the Brillouin zone pictured in the inset of Fig. 1(b)]. The shapes of the second-order spectra are determined by the two-magnon density of states weighted to account for the $\vec{k}$ dependence of the scattering interaction.

There are four basic two-magnon states for each pair of wave vectors $\vec{k}$ and $-\vec{k}$:

	S^z	Parity
$\|2,+\rangle=\|\uparrow\vec{k},\uparrow-\vec{k}\rangle$	2	+
$\|0,+\rangle=\|\uparrow\vec{k},\downarrow-\vec{k}\rangle+\|\downarrow\vec{k},\uparrow-k\rangle$	0	+
$\|0,-\rangle=\|\uparrow\vec{k},\downarrow-\vec{k}\rangle-\|\downarrow\vec{k},\uparrow-k\rangle$	0	−
$\|-2,+\rangle=\|\downarrow\vec{k},\downarrow-\vec{k}\rangle$	−2	+

The state $|0,-\rangle$ is responsible for the electric dipole two-magnon absorption.[3] It is important to determine which of the positive-parity states contribute to the two-magnon Raman scattering. The $S^z=\pm2$ two-magnon states involve excitation of two magnons on the same sublattice, and would have their energies shifted by an applied magnetic field at a rate of about ±0.2 cm^{-1}/kOe.[4] The $S^z=0$ state, on the other hand, is formed from one magnon on each sublattice and its energy should show no dependence on magnetic field. We have observed no change in the spectra of Fig. 1 in fields up to 50 kOe applied either parallel or perpendicular to the c axis. The same was found for the two-magnon peak in FeF_2. Thus

experimentally the $S^z = 0$ state is seen to be the important one for two-magnon scattering. The observed magnetic field behavior also rules out the previously mentioned possibility[1] that the scattering might be due to one magnon plus one phonon.

The first-order magnon scattering[1] is thought to occur by an indirect electric dipole interaction involving the spin-orbit interaction.[5,6] This mechanism also predicts a second-order scattering, but with an intensity much smaller than the first-order scattering, in disagreement with experiments on FeF_2.[1] Here we propose that the two-magnon scattering occurs by an excited-state exchange interaction similar to that invoked by Tanabe, Moriya, and Sugano[7] for the two-magnon absorption process. This appears to be a much stronger mechanism, and will be discussed in greater detail elsewhere[8,9]; here we outline the main features of the mechanism which pertain to the experimental results cited above. We emphasize that this mechanism does not contribute to one-magnon light scattering.

Let $\vec{E}_1$ and $\vec{E}_2$ be the electric vectors of the incident and scattered light waves, and consider two representative ions i and j on the two sublattices. We suppose that in the ground state ion i (j) has an electron with coordinate $\vec{r}_1$ ($\vec{r}_2$) and $S^z = \frac{1}{2}$ ($-\frac{1}{2}$) in an orbital φ_i (φ_j). The matrix element for a Raman process accompanied by simultaneous spin transitions of ions i and j can be written

$$M_{ij} = \left\{ \sum_{\mu\nu} \frac{\langle \varphi_j{\uparrow} | e\vec{E}_2 \cdot \vec{r}_1 | \varphi_\nu{\uparrow} \rangle V_{ij}^{\nu\mu} \langle \varphi_\mu{\uparrow} | e\vec{E}_1 \cdot \vec{r}_1 | \varphi_i{\uparrow} \rangle}{(E_\nu - \hbar\omega_1)(E_\mu - \hbar\omega_1)} + 11 \text{ similar terms} \right\} S_i^- S_j^+ . \tag{1}$$

The 11 similar terms have different ordering of operators or r_1 replaced by r_2. Here φ_ν and φ_μ are excited odd-parity electronic states with energies E_ν and E_μ, ω_1 is the incident frequency, and $V_{ij}^{\nu\mu} = \langle \varphi_i{\downarrow} \varphi_\nu{\uparrow} | e^2/|\vec{r}_1 - \vec{r}_2| \, \varphi_j{\downarrow} \varphi_\mu{\uparrow} \rangle$.

The above matrix element must now be summed over all pairs of ions i and j on the two sublattices taking account of the symmetry of the lattice. If the sum is restricted to nearest-neighbor pairs of spins on opposite sublattices, it can be shown by group theory[10] that the spin Hamiltonian for the Raman process in which one magnon is excited on each of the sublattices has the form

$$\begin{aligned} H_s = \sum_{\langle i,j \rangle} \{ & A(E_1^x E_2^x + E_1^y E_2^y) + BE_1^z E_2^z + C(E_1^x E_2^y + E_1^y E_2^x)\sigma_{ij}^x \sigma_{ij}^y \\ & + D[(E_1^y E_2^z + E_1^z E_2^y)\sigma_{ij}^y \sigma_{ij}^z + (E_1^z E_2^x + E_1^x E_2^z)\sigma_{ij}^z \sigma_{ij}^x] \\ & + F[(E_1^y E_2^z - E_1^z E_2^y)\sigma_{ij}^y \sigma_{ij}^z - (E_1^z E_2^x - E_1^x E_2^z)\sigma_{ij}^z \sigma_{ij}^x] \} S_i^- S_j^+ + \text{c.c.}, \end{aligned} \tag{2}$$

where A, B, C, D, and F are coupling constants like M_{ij} given by Eq. (1) with the electric fields and spin operators removed and appropriate components of $\vec{r}_1$ and $\vec{r}_2$ inserted; $\alpha_{ij}^\alpha = \mathrm{sgn}(\vec{r}_i - \vec{r}_j)_\alpha$, where $\alpha = x, y, z$, determines the relative phases with which the contributions of the j neighbors of a given spin i are to be combined.

The spin operators S_i^- and S_j^+ in (2) can now be transformed into magnon operators in the usual way[11] and the extinction coefficient calculated by time-dependent perturbation theory. For example, the term proportional to C gives rise to an extinction coefficient

$$\begin{aligned} h^{xy} = {} & (64S^2 \eta_2 \omega_1 \omega_2^3 C^2 / V \eta_1 c^4)(\epsilon_1^x \epsilon_2^y + \epsilon_1^y \epsilon_2^x)^2 \\ & \times \textstyle\sum_{\vec{k}} (n_{\vec{k}} + 1)^2 (u_{\vec{k}}^2 + v_{\vec{k}}^2)^2 \sin^2 \tfrac{1}{2} k_x a \sin^2 \tfrac{1}{2} k_y a \cos^2 \tfrac{1}{2} k_z c \, \delta(\omega_1 - \omega_2 - 2\omega_{\vec{k}}), \end{aligned} \tag{3}$$

where S is the ionic ground-state spin, η_1 and η_2 are the refractive indices for the incident and scattered light waves having frequencies ω_1 and ω_2 and polarization vectors $\vec{\epsilon}_1$ and $\vec{\epsilon}_2$, V is the crystal volume, $n_{\vec{k}}$ is the thermal magnon population number, $u_{\vec{k}}$ and $v_{\vec{k}}$ express the fraction of the magnon excitation residing on each sublattice,[11] and a and c are the lattice constants. Equation (3) shows clearly the dependence of the extinction coefficient on the magnon density of states determined by the delta function. The unweighted density of states has been illustrated by Allen, Loudon, and Richards.[3] We emphasize that the excited-state exchange mechanism proposed here predicts no scattering from the $S^z = \pm 2$ two-magnon states, in agreement with experiment.

The spectra calculated using Eq. (3) and similar expressions for the other polarizations appear as short dashed lines in Fig. 1. Especially in the "xz" case, agreement with experiment is improved by taking an extended range of excited-state exchange interaction between the ions i and j on opposite sublattices.[12] Since the excited-state wave functions are more spread out, the exchange matrix element for the excited state falls off more slowly with distance than for the ground state. If we assume an exponential fall-off as $\exp(-|\vec{r}_j - \vec{r}_i|/r_0)$ for the coupling, we calculate the second-order spectra indicated by the long dashed lines in Fig. 1 using a range parameter $r_0 \approx 0.4a$. The anisotropy fields and first-, second-, and third-neighbor exchange constants used here are $H_A = 1.05°\mathrm{K}$, $J_1 = 0.35°\mathrm{K}$, $J_2 = -1.735°\mathrm{K}$, and $J_3 = -0.025°\mathrm{K}$ and are consistent with the neutron-scattering data of Okazaki, Turberfield, and Stevenson.[13]

The theory is seen to predict correctly the peak positions and general shapes—i.e., symmetry versus pronounced asymmetry—of the "xy" and "xz" spectra. The unillustrated "xx" spectrum is also correctly predicted to be broad and featureless.

The particular critical-point features of the magnon density of states which are emphasized by the weighting functions for different experimental geometries can be predicted by group theory[8,9] irrespective of the nature of the Raman-scattering interaction. For "xy" the peak position indicates the magnon frequency at the point M. The R-point frequency is obtained from the cutoff in the "xz" spectrum. Combining this information with the frequency at Γ determined by first-order Raman scattering, one has enough information to obtain the magnon dispersion relation for crystals where this is not already known.[8]

Finally, the relative extinction coefficient for two-magnon and one-magnon scattering may now be estimated assuming the latter proceeds via spin-orbit coupling.[5,6] The result is[8,9]

$$\frac{h_2}{h_1} \simeq \frac{128 S V_{ij}^{\,2} E_0^{\,2}}{(u_0 + v_0)^2 \lambda^2 (\hbar\omega_1)^2}, \tag{4}$$

where λ is the excited-state spin-orbit coupling and E_0 is the excited-state energy. Evaluating for MnF_2, Eq. (4) gives $h_2/h_1 \simeq V_{ij}^{\,2}/10$ (with V_{ij} in cm^{-1}), using[14] $\lambda = 1000\ \mathrm{cm}^{-1}$. Because of the low frequency of the zone-center magnon ($\sim 8\ \mathrm{cm}^{-1}$), we have not observed one-magnon scattering in MnF_2. However, we may roughly test the theory for FeF_2, where Eq. (4) predicts $h_2/h_1 \simeq V_{ij}^{\,2}/60$. Together with the observed ratio $h_2/h_1 \simeq 2$, this implies $V_{ij} \simeq 10\ \mathrm{cm}^{-1}$. This is the same value obtained by Tanabe, Moriya, and Sugano[7] for the similar excited-state exchange controlling two-magnon absorption in FeF_2.

We thank B. B. Cetlin and C. A. Lambert for programming assistance, H. J. Guggenheim for the single crystals of MnF_2 and FeF_2, D. Olson and H. L. Carter for technical assistance, and A. Albert for crystal polishing.

---

[1]P. A. Fleury, S. P. S. Porto, L. E. Cheesman, and H. J. Guggenheim, Phys. Rev. Letters 17, 84 (1966).

[2]In Ref. 1 it is stated that for the two-magnon process in FeF_2, the "xx" and "yy" components were much stronger than the "xy." This is an error due to a misorientation of that sample in the xy plane. The true relative strengths for the "xx" and "xy" components agree with the results for MnF_2 discussed here.

[3]S. J. Allen, Jr., R. Loudon, and P. L. Richards, Phys. Rev. Letters 16, 463 (1966).

[4]A value of $g = 2$ has been assumed.

[5]R. J. Elliott and R. Loudon, Phys. Letters 3, 189 (1963).

[6]Y. R. Shen and N. Bloembergen, Phys. Rev. 143, 372 (1966).

[7]Y. Tanabe, T. Moriya, and S. Sugano, Phys. Rev. Letters 15, 1023 (1965).

[8]P. A. Fleury and R. Loudon, to be published.

[9]R. Loudon, to be published.

[10]J. O. Dimmock and R. G. Wheeler, Phys. Rev. 127, 391 (1962).

[11]See, for example, C. Kittel, Quantum Theory of

Solids (John Wiley & Sons, Inc., New York, 1963), Chap. 4.

[12]The same procedure was found necessary in Ref. 2, to explain the detailed shapes of two-magnon absorption spectra.

[13]A. Okazaki, K. C. Turberfield, and R. W. H. Stevenson, Phys. Letters 8, 9 (1964).

[14]A. Kiel, private communication.

ENERGY BAND CHANGES IN PEROVSKITES DUE TO LATTICE POLARIZATION

J. R. Brews
Bell Telephone Laboratories, Murray Hill, New Jersey
(Received 28 February 1967)

Many perovskites are capable of a ferroelectric transition from a cubic to a tetragonal phase. This transition is accompanied by movements of the ions within a single unit cell relative to one another. This lattice polarization causes splitting and shifting of the critical points of the cubic band structure. Recently several authors[1,2] have suggested that a similar polarization may be caused by external electric fields, and a preliminary estimate of the magnitude of this effect has been made for the single critical point $X_5'^{\text{lower}} \rightarrow X_5$.

Here a more complete analysis of the polarization dependence of the Kahn-Leyendecker[3] LCAO band scheme for $SrTiO_3$ is considered. It takes into account the reduction of point group symmetry from O_h to C_{4v} which occurs when the ions are moved along an [010] direction. This lower symmetry allows some of the matrix elements between the tight-binding states to be nonzero which were zero in the undistorted situation. These new matrix elements which break the cubic symmetry are of two types. One of these is nonzero because of the changes that the displacements introduce in the cubic LCAO parameters $pp\pi$, $pp\sigma$, $pd\pi$, and $pd\sigma$. These changes were estimated by assuming, e.g., for $pd\pi$,

$$pd\pi = (pd\pi)_0 S/S_0,$$

where S is the overlap integral between Watson's analytic Hartree-Fock wave functions[4] and subscripts indicate evaluation for the cubic configuration. Further discussion of this approximation is referred to by Kahn and Leyendecker.[3] The other type arises because the lines joining various pairs of atoms are no longer mutually perpendicular. These matrix elements contain as a factor the cosine of the angle between bonds (an angle near $\frac{1}{2}\pi$) and so vanish as the bonds become orthogonal. All these matrix elements were evaluated in the two-center approximation of Slater and Koster.[5]

One result of the lower symmetry of the distorted case is that the X points and also the M points split into two sets for which the group of the wave vector is different. Taking the direction of the displacements as [010], the [100] and [001] X points are labled $X_\perp$ and the [101] M point is labeled $M_\perp$. The other points are labeled $X_\parallel$ and $M_\parallel$. It is then found that the lines $\Gamma \rightarrow X_\parallel$ and $M_\perp \rightarrow R$ have the full point group symmetry C_{4v} and hence have representations Δ_j and T_j. From $X_\perp \rightarrow M_\parallel$ the symmetry is C_{2v} and the representations are Z_j. For $\Gamma \rightarrow X_\perp$ and $X_\parallel \rightarrow M_\parallel$ the only symmetry operation aside from the identity is a single reflection plane—the xy or else the yz plane—and the representations are labeled G or U depending on whether they are even or odd under reflection. Symmetry then dictates the selection rules listed in Table I in the notation of Bouckaert, Smoluchowski, and Wigner and Hamermesh.[6]

Although the LCAO parameters used in Table I are for $SrTiO_3$, a very similar band structure should apply to $BaTiO_3$.[3] To gain some idea of the band structure for tetragonal $BaTiO_3$, the atomic displacements were chosen to correspond to this material.[7] The resulting band structure is compared with the cubic Kahn-Ley-

Table I. Selection rules dictated by the lower symmetry of the distorted case.

Polarization	Transition	Point
[100]	$\Delta_5 \leftrightarrow \Delta_1, \Delta_1', \Delta_2, \Delta_2'$	$\Gamma, X_\parallel$
	$T_5 \leftrightarrow T_1, T_1', T_2, T_2'$	$M_\perp$
	$Z_1 \leftrightarrow Z_3$	$M_\parallel$[110]
	$Z_2 \leftrightarrow Z_4$	$X_\perp$[100]
	$Z_1 \leftrightarrow Z_4$	$M_\parallel$[011]
	$Z_2 \leftrightarrow Z_3$	$X_\perp$[001]
[010]	Only between levels of the same symmetry type	All points